Supplemental Experimental Procedures

Animals

NIDA (ICSS and tetrode recording). Male and female cKO mice (*Slc17a6*$^{flox/flox}$; *Slc6a3*$^{+/IRESCre}$) (Birgner et al., 2010) and littermate control mice (*Slc17a6*$^{+/flox}$; *Slc6a3*$^{+/IRESCre}$) were used (3–5 month old; transferred from Uppsala University, Sweden and housed at NIDA animal facility). Male TH-Cre mice(Lindeberg et al., 2004) (3–5 month old; NIDA animal facility, NIH) were used. After surgery, they were singly housed and kept on a 12/12 h light/dark cycle and had *ad libitum* access to food and water except during testing. All procedures were approved by the Animal Care and Use Committee (ACUC) of the Intramural Research Program, National Institute on Drug Abuse and were in accordance with National Research Council's *Guide for the Care and Use of Laboratory Animals*.

Uppsala (Amperometry). Female cKO mice (*Slc17a6*$^{flox/flox}$; *Slc6a3*$^{+/IRESCre}$) and littermate control mice (*Slc17a6*$^{+/flox}$; *Slc6a3*$^{+/IRESCre}$) bred at Uppsala University, Sweden were used (Birgner et al., 2010). They were housed separated by sex in standard macrolon cages (59×38×20 cm) with aspen wooden bedding (Scanbur AB Sollentuna, Sweden) and cage enrichment. Mice were maintained in a temperature (21–22°C) and humidity (45–55%) controlled facility on a 12/12 h light/dark cycle. The animals had *ad libitum* access to food (R36, Labfor, Lactamin, Vadstena, Sweden) and water. All mice used were housed in the animal facility at Uppsala University, Uppsala, Sweden, in accordance with the Swedish regulation guidelines (Animal Welfare Act SFS 1998:56) and European Union legislation (Convention ETS123 and Directive 2010/63/EU). Ethical approval was obtained from the Uppsala Animal Ethical Committee.

UCSD (Place preference). Male and female cKO mice (*Slc17a6*$^{flox/flox}$; *Slc6a3*$^{+/IRESCre}$) and control mice (*Slc17a6*$^{+/flox}$; *Slc6a3*$^{+/IRESCre}$) were bred at UCSD (Backman et al., 2006; Hnasko et al., 2010). They were group housed and maintained on a 12-12h light-dark cycle with food and water available *ad libitum*. All experiments were conducted in accordance with protocols approved by the UCSD Institutional Animal Care and Use Committee.

Stereotaxic surgery

ICSS and tetrode recording. We used ketamine/xylazine mixture (~80/12 mg/kg, i.p.) for anesthesia. All mice (TH-Cre, control and cKO) received AAV viral vector injection and optical fiber (200-µm diameter) implantation in the VTA; some of the mice received a second surgery for electrodes implantation in the VStr. The University of Pennsylvania Penn Vector Core produced Cre-dependent AAV encoding ChR2, the pAAV-Ef1a-DIO-hChR2 (H134R)-EYFP-WPRE-hGH. The final viral concentration was 9×10^{12} GC (genome copies)/ml. The coordinates for VTA viral injections were AP –3.3 mm, ML 0.5 mm and DV 4.1 mm. AAV viral vectors (1 µl) were microinjected into the VTA with a syringe pump (Micro 4, World Precision Instruments) over 10 min, with additional 10 min before removal of the injection needle (34 gauge, beveled). An optic fiber (200-µm diameter) was then implanted 0.2 mm dorsal to the injection site, and was secured on the skull with stainless screws and dental cement.

Intracranial self-stimulation experiments were started three weeks after surgery, to allow sufficient time for viral gene expression. The coordinates for the VStr were AP 1.7 mm, ML 0.6 mm and DV 3.6 mm (from brain surface), tilted with a 7-degree angle with the electrode tip pointing toward the posterior brain (to avoid the lateral ventricle; Figure 2a). The electrode bundle (8 tetrodes; electrode tips were covered with a fluorescent dye, the *Invitrogen* Neurotrace Dil paste N22880, to mark the implantation track) was slowly lowered toward the VStr, and secured on the skull with stainless screws and dental cement. After about 3 days recovery from surgery, electrodes were screened for neural activity.

Amperometry. Mice were anesthetized with isoflurane (0.5-2 L/min, 1-3% v/v) and restrained in a stereotaxic apparatus. A unilateral injection of AAV2/5-ChR2 viral vector (AAV2.Ef1a.DIO.ChR2(H134R).eYFP.IRES (n=6), AV2.Ef1a.DIO.ChR2(H134R).mCherry.IRES (n=2) and AAV5.Ef1a.DIO.ChR2(H134R).eYFP.IRES (n=1) (1×10^{12} vector genome/mL, UNC Vector Core Facility, Chapel Hill, NC, USA) was made into the VTA using a NanoFil syringe with 35-gauge needle (World Precision Instruments, Sarasota, FL, USA). Injections were done at two dorsal-ventral (DV) levels at the following coordinates: AP –3.3 mm, ML 0.4 mm and DV (from the scull): 4.7 mm and 4.2 mm (injection rate: 0.10 μL/min, a total of 0.75 μL/coordinate). The stereotaxic coordinates for adults were determined using Paxinos and Watson brain atlas, fourth edition. The injection needle was left in place for 10 minutes after the last injection and then slowly removed. The animals were allowed to recover for at least 3 weeks before amperometry recordings were performed.

Place preference. Mice (11-16 weeks) were anesthetized with isoflurane and placed in a stereotactic frame (Kopf, 1900 model). Heads were leveled and holes drilled to inject virus into the VTA (coordinates in mm relative to Bregma: ML 0.3, AP –3.4, DV –4.4) and implant fiber optic cannula just dorsal to medial nucleus accumbens shell (coordinates in mm relative to Bregma: ML 0.5, AP 1.2, DV –3.8). Using a Hamilton syringe, 700 nl of AAV5-EF1a-DIO-ChR2-YFP (UNC vector core) was injected into the VTA and injector was left in place for at >10 minutes to minimize backflow up the needle track. Following infusion an optic fiber constructed from 200 μm core multimode optical fiber (FT200EMT, Thorlabs) inserted into a ceramic ferrule (Sparta et al., 2012) was implanted. Implants were stabilized using dental cement (Lang) secured by two skull screws (Plastics One). Animals were treated pre- and post-operatively with Carprofen (Pfizer, 5 mg/kg s.c.). Mice were monitored daily for signs of infection/distress and allowed to recover from surgery for 3-4 weeks prior to behavioral assay. Five days after final behavior session mice were deeply anesthetized with ketamine/xylazine and perfused transcardially with at least 10 ml phosphate buffered saline (PBS) followed by at least 20 ml 4% paraformaldehyde (PFA). Brains were cryoprotected in 30% sucrose until sunk, snap frozen, and 30–40 micron coronal cryosections cut, mounted on slides, and examined to confirm ChR2:YFP expression and implant placements. One animal from each of the control and cKO groups was discarded due to lack of native ChR2:YFP fluorescence in the NAc.

Intracranial self-stimulation (ICSS)

Mice were habituated to the self-stimulation chambers (Med. Associates) for two days, 30 min each day (baseline-phase). Two levers, an active and an inactive, were available in the

chamber. Press of the active lever triggered a 1-s flash of the cue light (Med. Associates), while press of the inactive level had no consequence. In the next 5- or 10-day acquisition-phase, mice were placed in the same chambers for 30 min each day, in which press of the active lever triggered 8 pulses of optogenetic stimulation in the VTA (no timeout except for the duration of optogenetic stimulation), while press of the inactive level had no consequence. We used 50-Hz optogenetic stimulation throughout the acquisition-sessions: a lower laser intensity (8 mW and 1-ms pulse width) was used between acquisition-sessions 1–5 (all three mouse lines), and a higher laser intensity (32 mW and 3-ms pulse width) was used between acquisition-sessions 6–10 (only control and cKO mice). This 50-Hz optogenetic stimulation parameter can trigger reliable action potentials of DA neurons *in vivo* (Ilango et al., 2014a), and it is also comparable to physiologically-relevant DA neuron activity in mice (Wang and Tsien, 2011).

Some of the top responders also received two additional 45-min self-stimulation sessions: the descending and ascending sessions, which were counter-balanced for the sequence at these two sessions. Each session consisted of three 15-min blocks; optogenetic stimulation parameters changed from 8 → 5 → 3 pulses (descending session), or from 3 → 5 → 8 pulses (ascending session) automatically at the end of each block without any cue indication. The inter-pulse intervals of the three optogenetic stimulation trains are 70 (3 pulses), 35 (5 pulses) and 20 (8 pulses) ms, respectively.

ICSS and DA receptor antagonists

TH-Cre mice were trained with ICSS (five sessions or more). When stable ICSS rates over 500 lever presses per session (30 min) were reached, mice received a habituation injection of saline 30 minutes before the next session to acclimate them to the IP injection procedure. Then on different sessions mice received saline, SCH (50 or 100 μg/kg), or sulpiride (50 mg/kg) 30 minutes before the ICSS session. The order of these injections was counterbalanced. A recovery-self-stimulation session was given in between the injection sessions.

***In vivo* electrophysiology**

We used a bundle of 8 tetrodes (32 channels) for *in vivo* recording in the VStr. The tetrode bundle was coupled with a movable (screw-driven) microdrive assembly (~1 g weight) (Wang et al., 2015). Each tetrode consisted of four wires (90% platinum and 10% iridium; 18-μm diameter with an impedance of ~1–2 MΩ for each wire; California Fine Wire). Neural signals were pre-amplified, digitized and recorded using a Neuralynx Digital Lynx acquisition system. Spikes were digitized at 32 kHz and filtered at 600–6,000 Hz, using one recording electrode that lacked obvious spike signals as the reference. The electrode bundle was lowered by ~80 μm after completing one or a few recording sessions (depending on the experimental procedure). One or several depths of recording in the VStr were performed in each mouse.

***In vivo* amperometry**

The microelectrode consisted of a ceramic paddle with four platinum recording sites (Konradsson-Geuken et al., 2009; Mishra et al., 2015). The sites were arranged in two pairs

beginning approximately 100 µm from the electrode tip. To design a glutamate sensitive microelectrode, one pair of recording sites was coated with a mixture of GluOx 2%, 0.5 unit/1 µL), BSA (1%) and glutaraldehyde (0.125%).The remaining pair was coated only with BSA (1%) and glutaraldehyde (0.125%) to serve as control (sentinel/background) channels, sensitive to the oxidation of all endogenous molecules other than glutamate. This selective coating of the microelectrode allows for a self-referenced recording in which the current derived exclusively from glutamate oxidation can be isolated (Day et al., 2006; Konradsson-Geuken et al., 2009; Mishra et al., 2015; Rutherford et al., 2007). Enzyme-coated microelectrodes were allowed to cure for at least 48 hours at room temperature before any further use. Briefly, the released glutamate is oxidized by GluOx at the glutamate-sensitive sites, generating α-ketoglutarate and H_2O_2. As the microelectrode is maintained at a constant potential (+0.7 V versus an Ag/AgCl reference electrode), the H_2O_2 reporting molecule is further oxidized, yielding two electrons. The resulting current is then amplified and recorded by a FAST-16 recording system (Quanteon, LLC, Nicholasville, KY, USA). Extracellular glutamate reaches the platinum surface of control sentinels (without GluOx), but no oxidation current is generated. Therefore, any current detected at these sites is due to electrochemically active molecules other than glutamate.

Prior to calibration *m*-PD (5.0 mM) was electropolymerized onto all sites of the microelectrode in order to reduce access of potential electroactive interferents, like AA and catecholamines, to the platinum recording sites (Day et al., 2006; Konradsson-Geuken et al., 2009; Mishra et al., 2015; Rutherford et al., 2007). The electroplating was done in nitrogen-saturated phosphate-buffered saline 0.05 M, using the FAST-16 electroplating tool (peak-to-peak amplitude of 0.25 V every 0.05 s for 22 minutes). Microelectrodes were calibrated *in vitro* immediately prior to implantation. Calibrations were performed in a stirred solution of phosphate-buffered saline (0.05 M, 40 mL, pH 7.4, 37°C). A stable baseline was established: AA (250 µM), three aliquots of glutamate (20 mM; resulting in to a final concentration of 20, 40 and 60 µM), DA (2 µM), and H_2O_2 (8.8 µM) were sequentially added to the calibration beaker. Amperometric signals were acquired at a rate of 10 Hz. The sensitivity (pA/µM glutamate), limit of detection (LOD) for µM glutamate concentration (i.e. the smallest signal in glutamate concentration detected), selectivity (ratio of glutamate over AA), and linearity (R^2) were calculated. The microelectrodes to be used for implantation and further *in vivo* recordings had to fulfill the following calibration criteria: (i) similar background current (i.e. less than 20 pA difference between the glutamate-sensitive and control sentinel channels), (ii) linear response to increasing concentrations of glutamate (R^2 close to 1), (iii) a minimum glutamate sensitivity of –0.003 nA/µM glutamate, (iv) a LOD of ≤0.5 µM, and (v) a high selectivity for glutamate over AA and DA (i.e. >50:1). None of the electrodes used responded to DA during the calibration. Among the electrodes used, the lowest selectivity for glutamate over AA was 126:1.

Glutamate recordings were performed under continuous anesthesia (isoflurane with air (30% O_2 and 70% N_2, 0,5–2 L/min, 1–3% v/v), maintained at a constant potential of +0.7 V. A microelectrode mounted with an optic fiber (200 µm in diameter, Thorlabs, Inc., Newton. NJ, USA) was unilaterally implanted in the VStr: AP 1.1, ML 0.52 mm, and DV 4.0 mm from dura. An Ag/AgCl reference electrode was implanted on the contralateral side inside a brain region distant from the recording area. Terminal glutamate release was recorded in the VStr using optic stimulation. The light stimulation was generated by a 473 nm MBL-III-473-100 mW laser

(CNI Lasers, Changchun, China) with a power output between 4 and 8 mW. Five subsequent light pulses, separated with 30 seconds were delivered (20Hz, 5ms pulses for 1s) via the 200 µm optical fiber, mounted on the glutamate-sensitive electrode. To control for possible laser-induced artifacts, glutamate was also recorded at a constant potential of +0.25V during the delivery of three to five subsequent light pulses as described above.

Materials used: L-ascorbic acid (AA), DA, L-glutamate (monosodium salt), glutaraldehyde [25% (w/v) in water], bovine serum albumin (BSA), *m*-phenylenediamine dihydrochloride (*m*-PD), hydrogen peroxide (H_2O_2) and sodium chloride (NaCl) were ordered from Sigma Aldrich Corp. (St. Louis, MO, USA). L-Glutamate oxidase (GluOx; EC 1.4.3.11) was purchased from Heamochrom Diagnostics AB. All solutions were prepared using deionized water.

Place preference

To assess preference for environments paired with optogenetic stimulation we used home built two-chamber acrylic apparatuses. One chamber was distinguished by black walls and punched metal flooring; the second chamber by grey walls and stiff metal mesh flooring. Overhead cameras and ANY-maze video tracking software (Stoelting) were used to monitor time spent in each compartment, distance traveled, and number of crossings. On day 1 (pre-test) mice naïve to apparatus were placed in the center and monitored for 25 minutes. Ferrule implants were used to tether mice to DPSS lasers (473 nm OEM lasers) via 50-µm core optical patch cables and optical rotary joints (Doric Lenses), but lasers were powered off during pre-test. Time spent in each chamber was assessed and mice were assigned active (i.e. optogenetic stimulation-paired) sides in an unbiased manner to balance the mean pre-test times spent in active and inactive chambers for each genotype. On days 2–4 (pairing) we tested for a real-time place preference using conditions identical to day 1 except upon head entry to the pre-defined active side, software triggered TTL-pulses to activate the laser (20 Hz, 10-ms pulse width, ~10 mW at fiber tip), which discontinued upon head exit. Day 5 (post-test) was identical to day 1, with laser powered off to test for a potential conditioned place preference.

In vitro slice recordings

Adult mice (9-12 weeks) were deeply anesthetized with pentobarbital (200 mg/kg i.p.; Virbac) and perfused intracardially with 10 ml ice-cold sucrose-artificial cerebrospinal fluid (ACSF) containing (in mM): 75 sucrose, 87 NaCl, 2.5 KCl, 7 $MgCl_2$, 0.5 $CaCl_2$, 1.25 NaH_2PO_4, 25 $NaHCO_3$ and continuously bubbled with carbogen (95% O_2 – 5% CO_2). Brains were extracted and 200-µm coronal slices were cut in sucrose-ACSF using a Leica Vibratome (vt1200). Slices were transferred to a perfusion chamber at 31ºC containing ACSF (in mM): 126 NaCl, 2.5 KCl, 1.2 $MgCl_2$, 2.4 $CaCl_2$, 1.4 NaH_2PO_4, 25 $NaHCO_3$, 11 glucose, continuously bubbled in carbogen. After at least 45 min recovery, slices were transferred to a recording chamber continuously perfused with ACSF (2-3 ml/min) maintained at 29-31ºC using an in-line heater. Patch pipettes (3.5-5.5 MΩ) were pulled from borosilicate glass (King Precision Glass) and for voltage-clamp recordings filled with internal recording solution containing (in mM): 120 $CsCH_3SO_3$, 20 HEPES, 0.4 EGTA, 2.8 NaCl, 5 TEA, 2.5 Mg-ATP, 0.25 Na-GTP, at pH 7.25 and 285 +/- 5 mOsm.

VTA terminals were visualized in the NAc shell by epifluorescence and visually-guided patch recordings were made using infrared-differential interference contrast (IR-DIC) illumination (Axiocam MRm, Examiner.A1, Zeiss). ChR2 was activated by flashing blue light (5-ms pulse) through the light path of the microscope objective using a light-emitting diode (UHP-LED460, Prizmatix) under computer control. Excitatory postsynaptic currents (EPSCs) were recorded in whole-cell voltage clamp mode (Multiclamp 700B amplifier, Axon Instruments), filtered at 2 KHz, digitized at 10 KHz (Axon Digidata 1550, Axon Instruments), and collected on-line using pClamp 10 software (Molecular Device). Series resistance and capacitance were electronically compensated prior to recordings. Series resistance and/or leak current were monitored during recordings and cells that showed > 25% change during recordings were considered unstable and discarded.

Neurons were held in voltage-clamp at -60 mV to record AMPAR EPSCs in whole cell configuration. For whole-cell voltage-clamp recordings, single-pulse (5-ms) photostimuli were applied every 55 sec and 10 photo-evoked currents were averaged per neuron per condition. DMSO stock solution of 6,7-dinitroquinoxaline-2,3-dione (DNQX, Sigma) was diluted 1000-fold in ACSF and bath applied at 10 μM. Current sizes were calculated by using peak amplitude from baseline.

Data analysis

Sample sizes were based on the authors' experience of similar experiments performed in our labs. Unless explicitly notified, all data collected were included for analyses.

Tetrode recording. Mice with tetrodes implanted outside of the ventral striatum (based on histology) were excluded from analysis. Analyses on electrophysiological data were based on the sample size of 8 TH-Cre (223 units), 6 control (93 units) and 6 cKO (112 units) mice. These numbers are generally considered as sufficient in conducting statistical analyses. We used multiple spike-sorting parameters (e.g., principle component analysis, energy analysis) of Plexon OfflineSorter for separation of recorded spike waveforms. Sorted spikes were processed and analyzed in NeuroExplorer (Nex Technologies) and Matlab (Mathworks, Inc.). Low-frequency firing neurons of 0.2 Hz or less were excluded from the analyses due to insufficient number of spikes. For z-score analysis, neural activity one second before the optogenetic stimulation was used as the baseline. Perievent histograms (bin size = 5 ms) were smoothed with a Gaussian filter (filter width = 3 bins). Response latency was defined as the latency of the first bin from at least five consecutive bins that exceeded the z-score of 2 (or –2 for inhibited neurons). Response latencies that were 10 ms or less (as calculated above) were recalculated based on unsmoothed perievent histograms (bin size = 5 ms): the latency of the first bin that exceeded the z-score of 2 (or –2) was defined as the final response latency.

Amperometry. The analysis of recorded raw data was performed using FAST analysis 6.1 program (Jason Burmeister Consulting, LLC, USA). Based on the *in vitro* calibration carried out immediately before the experiment, the recorded signal was converted from pA to μM glutamate. Baseline glutamate levels were calculated as a difference between the signal of an enzyme-coated recording site and a sentinel site without enzyme-coating (subtracted signal). As

electrical interference will be measured both in enzyme-coated and sentinel sites, while glutamate signals are only recorded as a result of oxidation on the enzyme-coated sites, subtracted signal was used for calculation of amplitudes to reduce noise levels. Statistical analysis was performed using custom-written scripts in R (The R Project for Statistical Computing, http://www.r-project.org). The average of three to five consecutive stimulations was used to obtain the parameters for glutamate release in each of the experiments. To measure the size of a possible laser artifact generated by optical stimulation, light-evoked responses during a holding potential of +0.25 V were measured. An average of three to five consecutive stimulations was used for each experiment. The mean of the artifact (amplitude at +0.25 V) was subtracted from the amplitude at +0.7 V to obtain the absolute amplitude of glutamate in µM for each animal. In n=2 cKO animals, no recordings at 0.25 V were obtained and the mean of the artifacts of the other (n=3) cKO animals was subtracted instead. As the glutamate response of each animal was calculated as a mean of several stimulations, we used the composite standard deviation as basis for the calculation of the SEM of the groups (cKO and control). The data was tested for normality using the Shapiro-Wilk test. As the data was normally distributed ($W = 0.93627$, $P = 0.5433$), an unpaired two-tailed t-test was used to analyze statistical differences between the two experimental groups.

Histology

After completion of the ICSS or tetrode recordings, mice were deeply anesthetized and intracardially perfused with PBS followed by 4% paraformaldehyde (PFA). The final electrode position was marked by passing a 20-s, 10-µA current using a linear constant current stimulus isolator (Neurolog System) through two selected tetrodes. Brains were removed and post-fixed in PFA for at least 24 h. Brains were sliced on a cryostat (50-µm coronal sections) or a vibratome (60-µm coronal sections). Sections were mounted with the Mowiol mounting medium mixed with DAPI (Vector Laboratories) for fluorescent microscopic examination of viral vector expression, optical fiber and electrodes placements.

References

Backman, C.M., Malik, N., Zhang, Y., Shan, L., Grinberg, A., Hoffer, B.J., Westphal, H., and Tomac, A.C. (2006). Characterization of a mouse strain expressing Cre recombinase from the 3' untranslated region of the dopamine transporter locus. Genesis *44*, 383-390.

Birgner, C., Nordenankar, K., Lundblad, M., Mendez, J.A., Smith, C., le Greves, M., Galter, D., Olson, L., Fredriksson, A., Trudeau, L.E*., et al.* (2010). VGLUT2 in dopamine neurons is required for psychostimulant-induced behavioral activation. Proceedings of the National Academy of Sciences of the United States of America *107*, 389-394.

Day, B.K., Pomerleau, F., Burmeister, J.J., Huettl, P., and Gerhardt, G.A. (2006). Microelectrode array studies of basal and potassium-evoked release of L-glutamate in the anesthetized rat brain. Journal of neurochemistry *96*, 1626-1635.

Hnasko, T.S., Chuhma, N., Zhang, H., Goh, G.Y., Sulzer, D., Palmiter, R.D., Rayport, S., and Edwards, R.H. (2010). Vesicular glutamate transport promotes dopamine storage and glutamate corelease in vivo. Neuron *65*, 643-656.

Ilango, A., Kesner, A.J., Broker, C.J., Wang, D.V., and Ikemoto, S. (2014). Phasic excitation of ventral tegmental dopamine neurons potentiates the initiation of conditioned approach behavior: parametric and reinforcement-schedule analyses. Front Behav Neurosci *8*, 155.

Konradsson-Geuken, A., Gash, C.R., Alexander, K., Pomerleau, F., Huettl, P., Gerhardt, G.A., and Bruno, J.P. (2009). Second-by-second analysis of alpha 7 nicotine receptor regulation of glutamate release in the prefrontal cortex of awake rats. Synapse *63*, 1069-1082.

Lindeberg, J., Usoskin, D., Bengtsson, H., Gustafsson, A., Kylberg, A., Soderstrom, S., and Ebendal, T. (2004). Transgenic expression of Cre recombinase from the tyrosine hydroxylase locus. Genesis *40*, 67-73.

Mishra, D., Harrison, N.R., Gonzales, C.B., Schilstrom, B., and Konradsson-Geuken, A. (2015). Effects of age and acute ethanol on glutamatergic neurotransmission in the medial prefrontal cortex of freely moving rats using enzyme-based microelectrode amperometry. PloS one *10*, e0125567.

Rutherford, E.C., Pomerleau, F., Huettl, P., Stromberg, I., and Gerhardt, G.A. (2007). Chronic second-by-second measures of L-glutamate in the central nervous system of freely moving rats. Journal of neurochemistry *102*, 712-722.

Sparta, D.R., Stamatakis, A.M., Phillips, J.L., Hovelso, N., van Zessen, R., and Stuber, G.D. (2012). Construction of implantable optical fibers for long-term optogenetic manipulation of neural circuits. Nat Protoc *7*, 12-23.

Wang, D.V., and Tsien, J.Z. (2011). Convergent processing of both positive and negative motivational signals by the VTA dopamine neuronal populations. PLoS ONE *6*, e17047.

Supplemental Figures

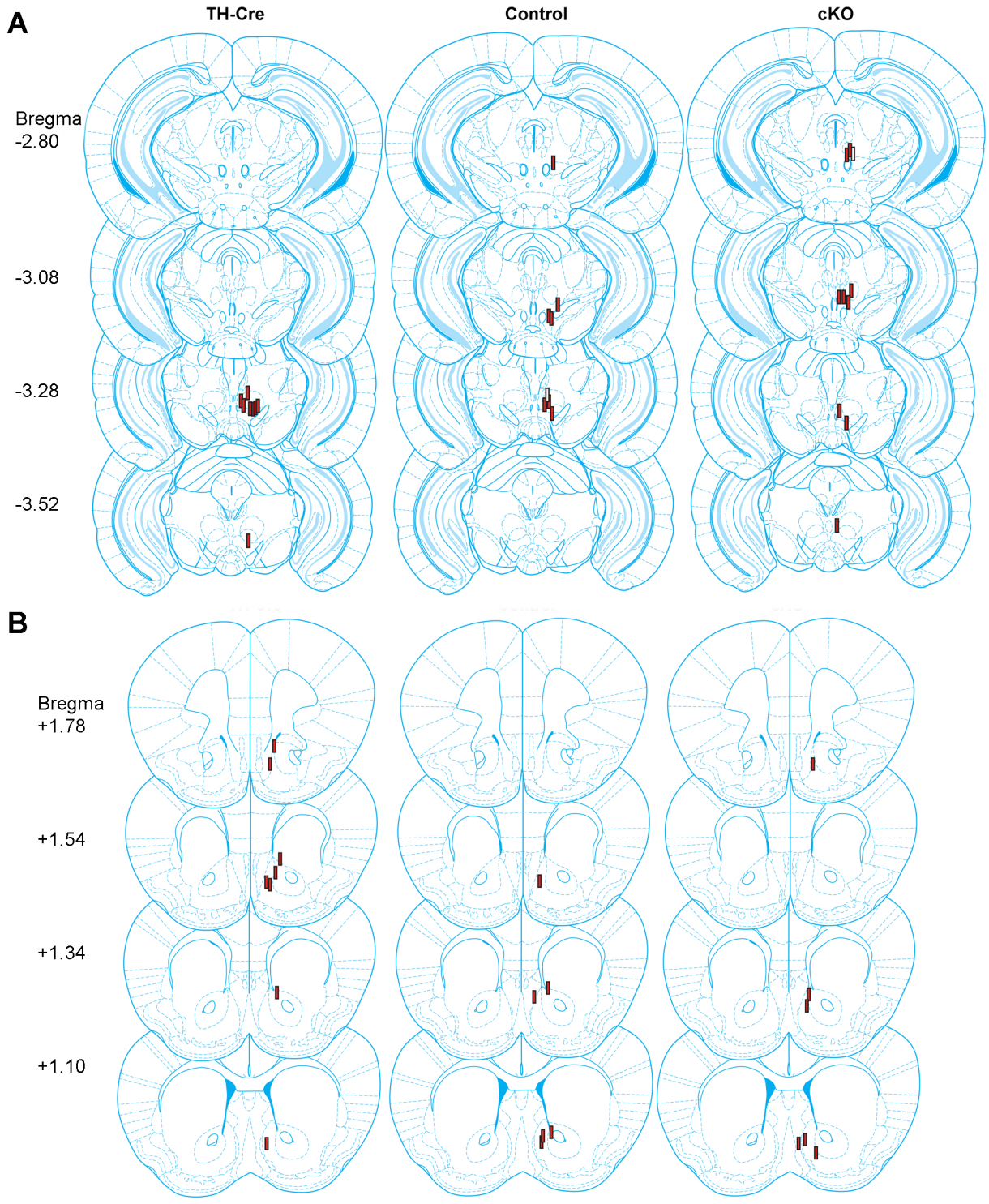

Figure S1. Optical fiber placements for individual TH-Cre (n = 10), control (n = 8) and cKO mice (n = 10), Related to Figures 1, 2 and 4

(A) Some of the fiber placements were not clear due to perfusion or sectioning issues and thus were not included here. Filled (red) squares are mice with good self-stimulation rate (500 times or above per 30 min); opens squares are mice with low self-stimulation rate (200 times or less per 30 min).

(B) Electrodes placements for individual TH-Cre (n = 8), control (n = 6) and cKO (n = 6) mice, from which the recorded single-unit activity was used for analyses

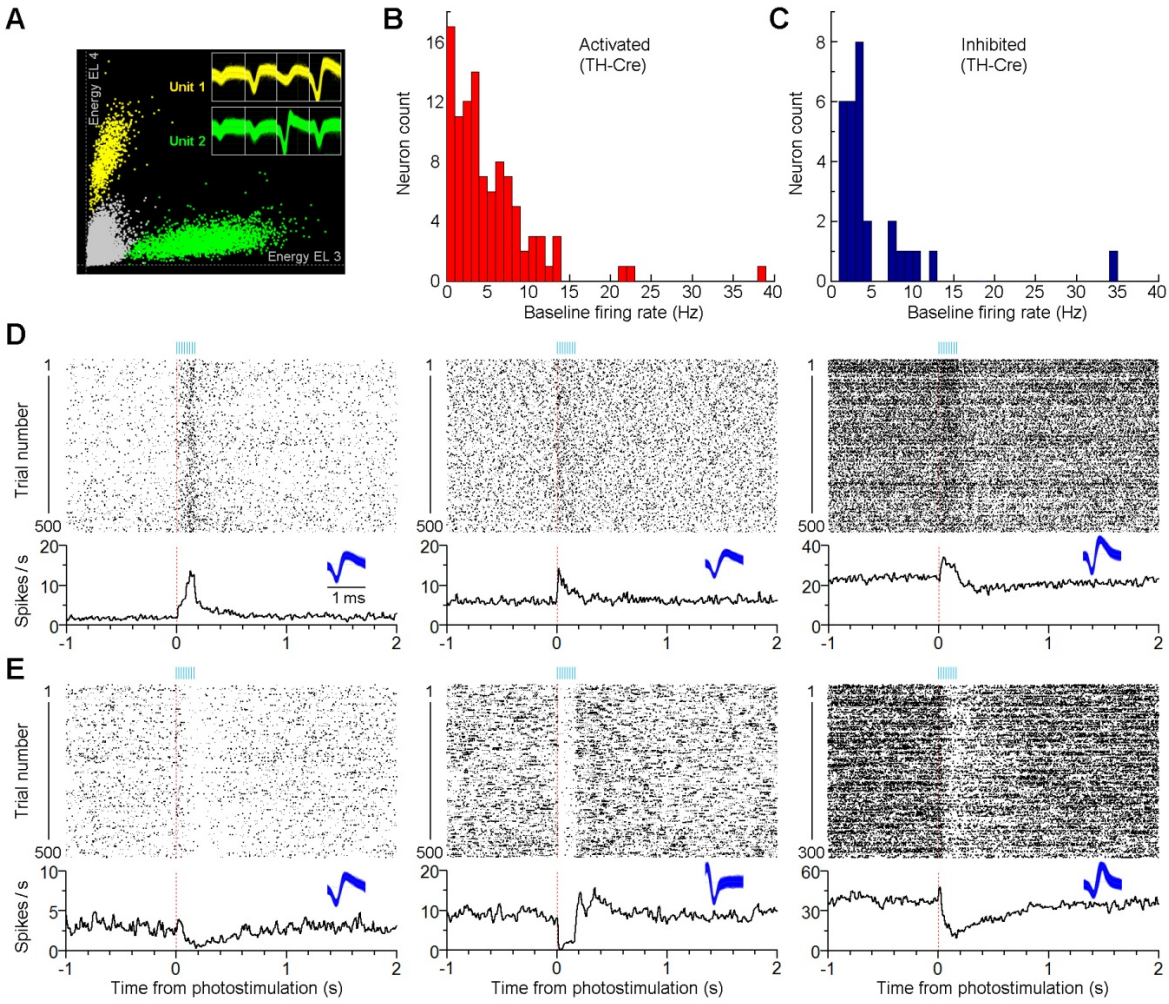

Figure S2. Optogenetic stimulation of VTA DA neurons evokes fast phasic response in both low- and high-frequency VStr neurons, Related to Figure 1

(A) An example of two sorted VStr units and their representative spike-waveforms (spike width, 1 ms) recorded from one tetrode. Spike sorting was conducted in Plexon OfflineSorter; each dot represents one spike waveform.

(B and C) Baseline firing distribution of the activated (B) and inhibited (C) VStr neurons upon optogenetic stimulation of DA neurons.

(D and E) Perievent rasters and histograms of representative activated (D) and inhibited (E) VStr neurons (n = 3 each) recorded in TH-Cre mice upon optogenetic stimulation of DA neurons. Insets, 1000 representative overlapping spike waveforms of the six neurons.

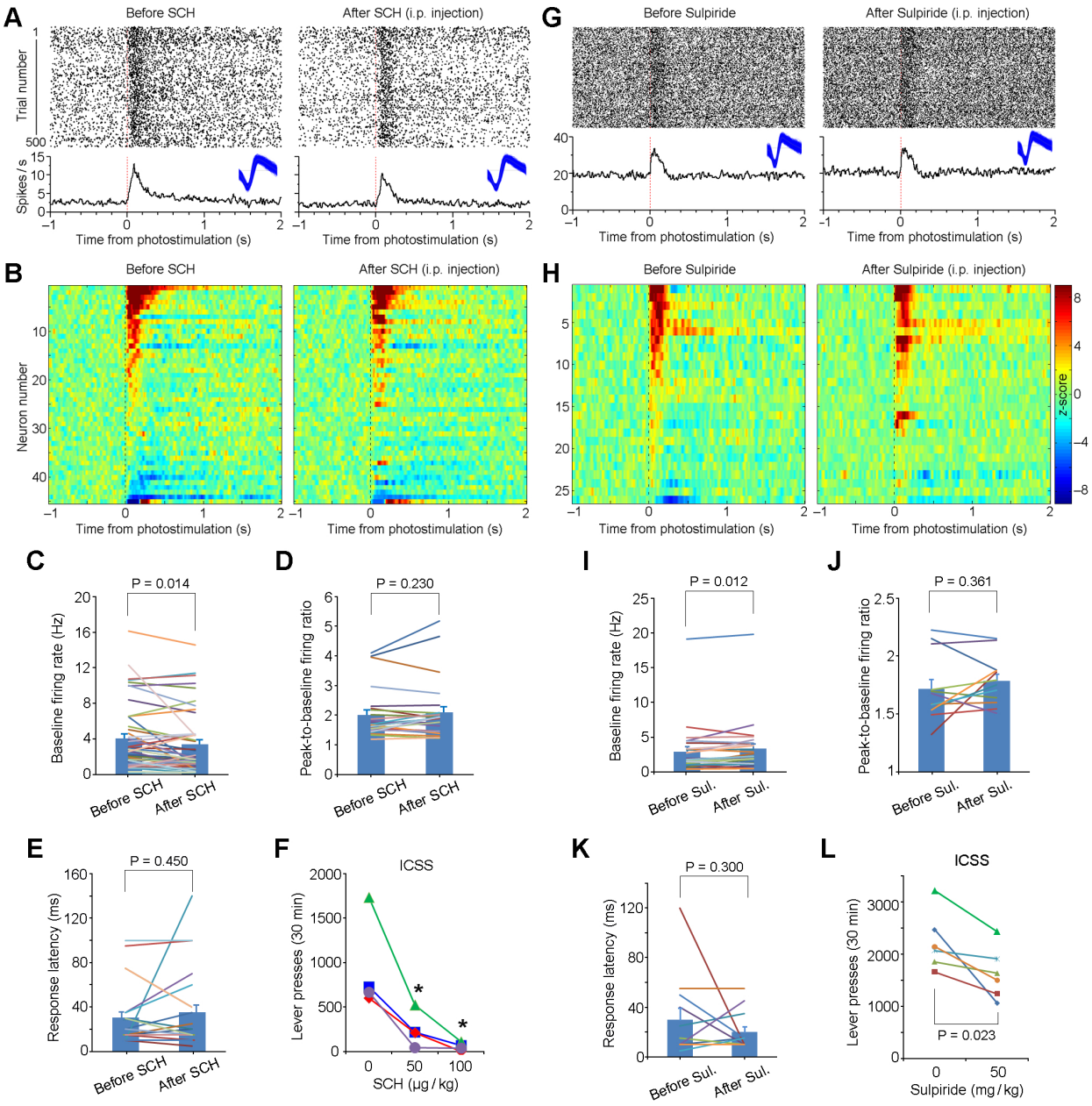

Figure S3. The D1 receptor antagonist SCH 23390 or D2 receptor antagonist Sulpiride decreases ICSS, but does not block fast phasic responses of VStr neurons in TH-Cre mice, Related to Figure 1

(A) Perievent rasters and histogram of a representative VStr neuron upon VTA optogenetic stimulation before (left panel) and after (right panel) SCH23390 (SCH) injection (50 μg/kg, i.p.). Insets, 1000 representative overlapping spike waveforms (blue traces; 1 ms) of the neuron.

(B) Summary of the z-scored perievent histogram of tested VStr neurons (n = 45) recorded in TH-Cre mice before (left panel) and after (right panel) SCH injection (50 or 100 μg/kg, i.p.).

Neurons are arranged in the same order in the left and right panels. Color bar represents z-scored firing frequency.

(C) SCH injections (50 μg/kg, i.p.) decreased baseline firing rates (Mean ± SEM; a paired two-tailed t-test performed for the same neurons #1–45 as shown in B).

(D) SCH injections (50 μg/kg, i.p.) did not alter difference between baseline rate (1 s before optogenetic stimulation) and peak firing rate (0–0.5 s after optogenetic stimulation) of neurons significantly excited by optogenetic stimulation (a paired two-tailed t-test).

(E) SCH injections (50 μg/kg, i.p.) did not alter response latency of neurons significantly excited by optogenetic stimulation.

(F) SCH injections (50 or 100 μg/kg, i.p.) significantly reduced ICSS rates (n = 4; $*P < 0.05$, Tukey posthoc test after a significant dose effect with one-way ANOVA: $F_{2,6} = 12.48$, $P = 0.0073$).

(G) Perievent rasters and histogram of a VStr neuron upon VTA optogenetic stimulation before (left panel) and after (right panel) Sulpiride (Sul) injection (50 mg/kg, i.p.). Insets, 1000 representative overlapping spike waveforms (blue traces; 1 ms) of the neuron.

(H) Summary of the z-scored perievent histogram of tested VStr neurons (n = 26) recorded in TH-Cre mice before (left panel) and after (right panel) Sul injections (50 mg/kg, i.p.). Neurons are arranged in the same order in the left and right panels. Color bar represents z-scored firing frequency.

(I) Sul injections (50 mg/kg, i.p.) slightly increased baseline firing rates (Mean ± SEM; a paired two-tailed t-test performed for the same neurons #1–26 as shown in B).

(J) Sul injections (50 mg/kg, i.p.) did not alter difference between baseline rate (1 s before optogenetic stimulation) and peak firing rate (0–0.5 s after optogenetic stimulation) of neurons significantly excited by optogenetic stimulation, evaluated with a paired two-tailed t-test.

(K) Sul injections (50 mg/kg, i.p.) did not alter response latency of neurons significantly excited by optogenetic stimulation.

(L) Injections of Sul (50 mg/kg, i.p.) significantly decreased ICSS rates (n = 6).

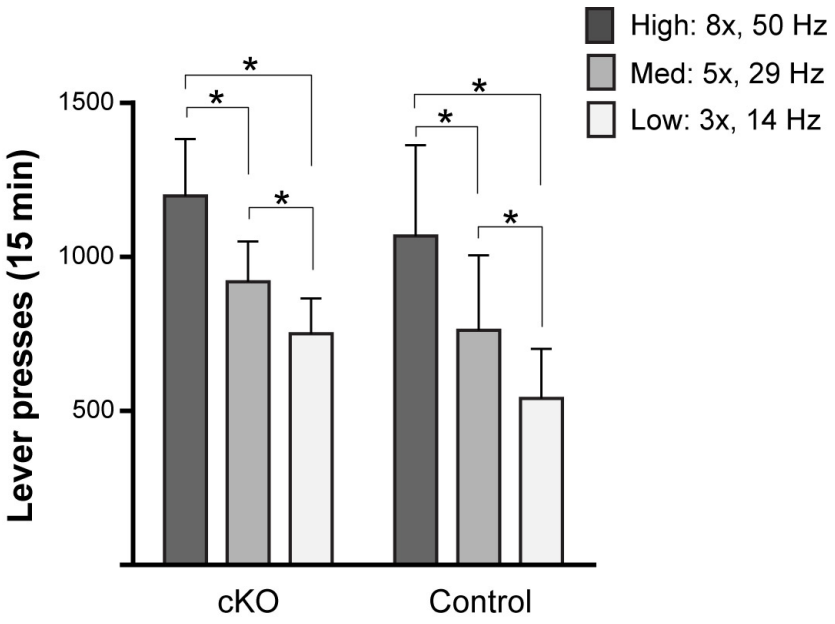

Figure S4. Parametric study of the VTA DA neuron-mediated ICSS, Related to Figure 4

Mice received three different values of optogenetic stimulation consisting of 3, 5 and 8 pulses with different frequencies in such a way that the three trains had the same duration (0.14 s). Effects of the three trains were examined in three 15-min blocks with ascending and descending orders over two sessions (45 min/session); the order of testing with the ascending and descending orders was counterbalanced among the mice of each group. All mice displayed ICSS responses dependent on reward-value. Because the effect of ascending and descending orders was not significant for all three strains, the mean ICSS data are presented as a function of stimulation value with order factor collapsed together. The cKO mice responded at different rates as a function of optogenetic stimulation value ($n = 7$; $F_{2,12} = 6.75$, $p < 0.001$ with a 2_{order} x $3_{stimulation\ value}$ ANOVA), while control displayed similar ICSS responses ($n = 3$; $F_{2,4} = 33.46$, $p < 0.005$ with a 2_{order} x $3_{stimulation\ value}$ ANOVA). Error bars, SEM.

Table S1. Raw data of glutamate release, Related to Figure 3

ID	Genotype	sex	LaserPower (mW)	Voltage (V)	length (s)	Amplitude (μM)
0.7 V (glutamate response)						
1	Control	Female	4	0.7	1	0.5592
1	Control	Female	4	0.7	1	0.3716
1	Control	Female	4	0.7	1	0.4952
1	Control	Female	4	0.7	1	0.3365
1	Control	Female	4	0.7	1	0.4057
2	Control	Female	4	0.7	1	0.5719
2	Control	Female	4	0.7	1	0.4779
2	Control	Female	4	0.7	1	0.5005
2	Control	Female	4	0.7	1	0.5323
2	Control	Female	4	0.7	1	0.5607
3	Control	Female	8	0.7	1	0.7391
3	Control	Female	8	0.7	1	0.7464
3	Control	Female	8	0.7	1	0.7309
3	Control	Female	8	0.7	1	0.8096
3	Control	Female	8	0.7	1	0.7723
4	cKO	Female	8	0.7	1	0.2129
4	cKO	Female	8	0.7	1	0.3676
4	cKO	Female	8	0.7	1	0.2835
4	cKO	Female	8	0.7	1	0.1681
4	cKO	Female	8	0.7	1	0.4596
5	cKO	Female	7	0.7	1	0.3151
5	cKO	Female	7	0.7	1	0.3194
5	cKO	Female	7	0.7	1	0.3102
5	cKO	Female	7	0.7	1	0.3070
5	cKO	Female	7	0.7	1	0.3405
6	cKO	Female	6	0.7	1	0.3472
6	cKO	Female	6	0.7	1	0.3947
6	cKO	Female	6	0.7	1	0.4037
6	cKO	Female	6	0.7	1	0.3830
6	cKO	Female	6	0.7	1	0.4142
7	cKO	Female	4	0.7	1	0.2102
7	cKO	Female	4	0.7	1	0.0652
7	cKO	Female	4	0.7	1	0.2848
8	cKO	Female	4	0.7	1	0.3367
8	cKO	Female	4	0.7	1	0.6323
8	cKO	Female	4	0.7	1	0.3542
8	cKO	Female	4	0.7	1	0.4431
8	cKO	Female	4	0.7	1	0.4845

Table S1 – continues

9	Control	Female	4	0.7	1	1.6112
9	Control	Female	4	0.7	1	1.5361
9	Control	Female	4	0.7	1	1.5342
9	Control	Female	4	0.7	1	1.5430
9	Control	Female	4	0.7	1	1.4980
0.25 V (artifact values)						
1	Control	Female	4	0.25	1	0.0638
1	Control	Female	4	0.25	1	0.1187
1	Control	Female	4	0.25	1	0.0469
2	Control	Female	4	0.25	1	0.3039
2	Control	Female	4	0.25	1	0.2120
2	Control	Female	4	0.25	1	0.2796
3	Control	Female	8	0.25	1	0.2417
3	Control	Female	8	0.25	1	0.2348
3	Control	Female	8	0.25	1	0.2448
5	cKO	Female	7	0.25	1	0.1276
5	cKO	Female	7	0.25	1	0.1462
5	cKO	Female	7	0.25	1	0.1399
7	cKO	Female	4	0.25	1	0.0716
7	cKO	Female	4	0.25	1	0.1978
7	cKO	Female	4	0.25	1	0.2115
7	cKO	Female	4	0.25	1	0.0278
8	cKO	Female	4	0.25	1	0.0866
8	cKO	Female	4	0.25	1	0.1527
8	cKO	Female	4	0.25	1	0.1722
8	cKO	Female	4	0.25	1	0.3346
8	cKO	Female	4	0.25	1	0.1529
9	Control	Female	4	0.25	1	1.0919
9	Control	Female	4	0.25	1	1.0199
9	Control	Female	4	0.25	1	1.0755
9	Control	Female	4	0.25	1	1.0381
9	Control	Female	4	0.25	1	0.9540

Table S2. Mean of each animal, Related to Figure 3

ID	Genotype	N stimulations)	Voltage (V)	Amplitude (µM)	sd	se	corrected amplitude (µM)
0.7 V (glutamate response)							
1	Control	5	0.7	0.4336	0.0917	0.0410	0.3572
2	Control	5	0.7	0.5287	0.0396	0.0177	0.2635
3	Control	5	0.7	0.7596	0.0320	0.0143	0.5192
4	cKO	5	0.7	0.2984	0.1176	0.0526	0.1501
5	cKO	5	0.7	0.3184	0.0132	0.0059	0.1805
6	cKO	5	0.7	0.3886	0.0258	0.0115	0.2403
7	cKO	3	0.7	0.1867	0.1117	0.0645	0.0596
8	cKO	5	0.7	0.4502	0.1188	0.0531	0.2704
9	Control	5	0.7	1.5445	0.0412	0.0184	0.5086
0.25 V (artifact values)							
1	Control	3	0.25	0.0764	0.0375	0.0217	
2	Control	3	0.25	0.2652	0.0476	0.0275	
3	Control	3	0.25	0.2404	0.0051	0.0030	
5	cKO	3	0.25	0.1379	0.0095	0.0055	
7	cKO	4	0.25	0.1272	0.0914	0.0457	
8	cKO	5	0.25	0.1798	0.0924	0.0413	
9	Control	5	0.25	1.0359	0.0540	0.0241	